

## Article

# Sphalerite Composition in Low- and Intermediate-Sulfidation Epithermal Ore Bodies from the Roșia Montană Au-Ag Ore Deposit, Apuseni Mountains, Romania

Călin Gabriel Tămaș<sup>1,2</sup>, Mădălina Paula Andrii<sup>1,\*</sup>, Réka Kovács<sup>1</sup>, Sergiu Drăgușanu<sup>1</sup> and Béatrice Cauuet<sup>2</sup>

<sup>1</sup> Department of Geology, Faculty of Biology and Geology, Babeș-Bolyai University, 1, M. Kogălniceanu Street, 400084 Cluj-Napoca, Romania; calin.tamas@ubbcluj.ro (C.G.T.); kovacsreka056@gmail.com (R.K.); dragusanusergiu@yahoo.com (S.D.)

<sup>2</sup> TRACES Laboratory, UMR 5608-CNRS, Toulouse Jean-Jaurès University, TRACES-CNRS, 5, A. Machado Street, 31058 Toulouse, France; beatrice.cauuet@univ-tlse2.fr

\* Correspondence: madalina.andrii@ubbcluj.ro

**Abstract:** We evaluated the significance of the iron and manganese content in sphalerite as a tool for distinguishing between low-sulfidation and intermediate-sulfidation epithermal deposits on the basis of new and previously published electron probe microanalyses data on the Roșia Montană epithermal ore deposit and available microchemical data from the Neogene epithermal ore deposits located in the Apuseni Mountains and Baia Mare region, Romania. Two compositional trends of the Fe vs. Mn content in sphalerite were delineated, a Fe-dominant and a Mn-dominant, which are poor in Mn and Fe, respectively. The overlapping compositional range of Fe and Mn in sphalerite in low-sulfidation and intermediate-sulfidation ores suggests that these microchemical parameters are not a reliable tool for distinguishing these epithermal mineralization styles.

**Keywords:** sphalerite; Roșia Montană; epithermal; low-sulfidation; intermediate-sulfidation



**Citation:** Tămaș, C.G.; Andrii, M.P.; Kovács, R.; Drăgușanu, S.; Cauuet, B. Sphalerite Composition in Low- and Intermediate-Sulfidation Epithermal Ore Bodies from the Roșia Montană Au-Ag Ore Deposit, Apuseni Mountains, Romania. *Minerals* **2021**, *11*, 634. <https://doi.org/10.3390/min11060634>

Academic Editors: Gheorghe Damian, Andrei Buzatu and Andrei Ionuț Apopei

Received: 28 April 2021

Accepted: 9 June 2021

Published: 15 June 2021

**Publisher's Note:** MDPI stays neutral with regard to jurisdictional claims in published maps and institutional affiliations.



**Copyright:** © 2021 by the authors. Licensee MDPI, Basel, Switzerland. This article is an open access article distributed under the terms and conditions of the Creative Commons Attribution (CC BY) license (<https://creativecommons.org/licenses/by/4.0/>).

## 1. Introduction

Two styles of epithermal ore deposits were distinguished in the late 1980s under the names adularia-sericite and acid-sulfate [1] or low- and high-sulfidation [2], respectively. Both terminologies were used in parallel for more than a decade and afterward low-sulfidation (LS) and high-sulfidation (HS) gradually became the usual terms employed. However, a third epithermal ore deposit style, named intermediate-sulfidation (IS), was distinguished from the previously considered low-sulfidation epithermal style in the late 1990s–early 2000s by the authors in [3] based on a review of the epithermal ore deposits in the northern Great Basin (USA) made by the researchers in [4].

Among the numerous distinguishing criteria between LS and IS deposits, one is the abundance and the composition of the sphalerite. This mineral tends to be uncommon or locally minor, Fe-rich, and compositionally zoned in LS ores, whereas, in IS deposits, it is common, Fe-poor, and compositionally homogeneous [3,5].

The Roșia Montană Au-Ag epithermal ore deposit from the South Apuseni Mountains (Romania) consists of both low-sulfidation and intermediate-sulfidation ore bodies characterized by specific ore and gangue mineral assemblages, hydrothermal fluid composition (salinities and homogenization temperatures), and distinct crosscutting and timing relationships [6]. Previously published and new electron probe microanalyses data on the Roșia Montană ore deposit facilitate the evaluation of the content range of Fe and Mn in sphalerite from both LS and IS ores.

The Baia Mare Neogene ore district in north-western Romania hosts tens of Pb–n-Cu ± Au–Ag epithermal deposits [7–9]. These ore deposits were previously considered as low-sulfidation [10,11]. This interpretation is updated for several ore deposits and the published microchemical data on sphalerite from these deposits are compared with the data

from Roșia Montană aiming to reconsider the significance of the sphalerite composition, i.e., the Fe and the Mn content as a distinguishing feature between the LS and IS epithermal ore deposit styles.

## 2. Geological Setting

### 2.1. The Apuseni Mountains

The Apuseni Mountains are located in the inner part of the Carpathian chain and are divided in two major units due to their pre-Neogene geological evolution [12–19], i.e., the North Apuseni Mountains (NAM) and the South Apuseni Mountains (SAM), respectively. The NAM are composed of the Bihor Unit, the Codru nappe system and the Biharia nappe system. The SAM are composed of Transylvanides units, which consist of an ophiolitic complex and related sedimentary rocks [14].

Several magmatic/volcanic events are spread within the Apuseni Mountains [20] (Figure 1a), i.e., Middle Jurassic mafic rocks (gabbros, basalt sheeted dykes, and pillow lavas) in the SAM; Lower Cretaceous calc-alkaline volcanism related to an island arc setting (basalts to rhyolites) in the SAM; Upper Cretaceous–Paleocene (mainly granodiorites) related to a continental subduction in both the NAM and SAM; and the so-called Neogene calc-alkaline to alkaline volcanism (andesitic-dacitic) set up in an extensional tectonic setting and restricted to the SAM (Miocene–Quaternary).

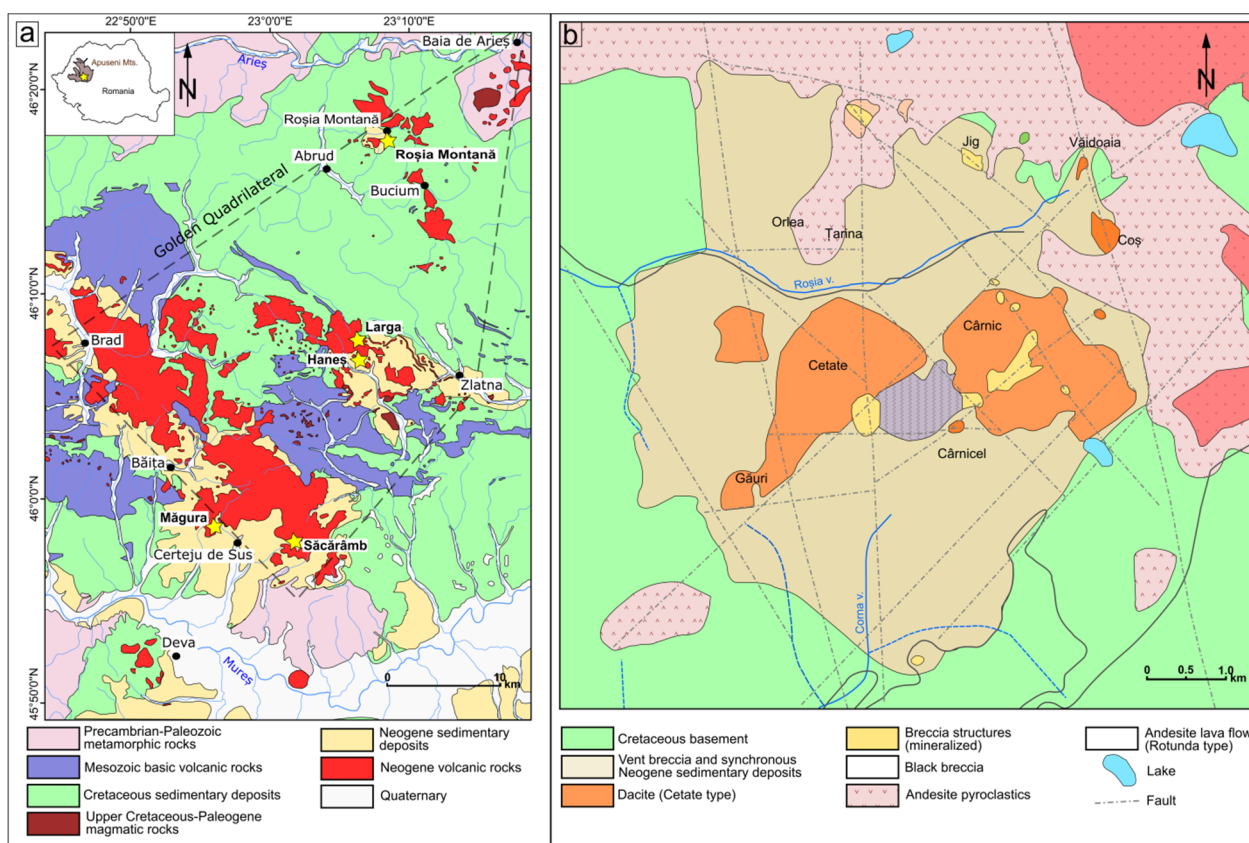


**Figure 1.** General geology data: (a) simplified geology of the South Apuseni Mountains (SAM) and the location of the ore deposits with published data on sphalerite (modified after [21,22]; and (b) geological map of the Roșia Montană ore deposit (modified after [23]).

The Neogene volcanic activity in SAM is concentrated along three main extensional basins heading NNW-SSE, namely Brad-Săcărâmb, Stănița-Zlatna, and Roșia Montană-Bucium, along with another two small-sized occurrences at Baia de Arieș and Deva [9,24]. The Neogene volcanic activity mainly generated andesites (Zarand, Bucium, Brad, Zlatna,

Baia de Arieș, and Săcărâmb), subordinately dacites (Roșia Montană), basaltic andesites (Detunata), and trachyandesites (Săcărâmb and Uroi) [25].

Field observations, geochemical analyses, and K-Ar ages [26] indicated that the Neogene volcanic activity started in newly created pull-apart basins with volcanogenic sedimentation followed by a calc-alkaline volcanic event (14.8–11 Ma) in the Zarand-Barza-Zlatna-Roșia Montană-Bucium areas and a subsequent adakite-like calc-alkaline event (12.6–7.4 Ma) in the Deva-Săcărâmb-Hărtăgani and Baia de Arieș-Roșia Montană areas. Subordinately, alkaline volcanic rocks were emplaced in the Săcărâmb-Hărtăgani area (10.5 Ma), and at Bucium (7.4 Ma). The last volcanic event (1.6 Ma) occurred at Uroi [25].

The South Apuseni Mountains are the most important ore province in the Carpathian chain [27] with Neogene epithermal and porphyry ore deposits concentrated in an area known as the Golden Quadrilateral [24,28]. Two types of porphyry deposits are known in the Apuseni Mountains, Cu-Au (e.g., Roșia Poieni; [29]) and Au-Cu (Bolcana; [30]). Tens of epithermal ore deposits occur as well [8,9,31] mostly of an IS type [6,32]; however, according to the available geological data, LS and HS deposits also occur, e.g., (i) the largest Au-rich ore bodies from Roșia Montană, and the collapsed breccia host Au-ores from Baia de Arieș and (ii) Pârâul lui Avram and Larga, respectively.

## 2.2. The Roșia Montană Ore Deposit

The Roșia Montană ore deposit is located in the northern part of the Golden Quadrilateral, in the SAM (Figure 1b). This deposit hosts an identified resource of approximately 400 Mt of ore at an average grade of 1.3 g/t Au and 6 g/t Ag, which makes it the largest gold deposit in Europe, with a total resource of 16.1 Moz Au and 73.3 Moz Ag [33].

The basement of the Roșia Montană area is formed of Upper Cretaceous flysch with shales and sandstones, which outcrops around the ore deposit. The crystalline basement that is exposed towards the north in the Baia de Arieș area occurs at Roșia Montană only as fragments within different breccia pipe structures [12,34,35]. The Neogene volcanic rocks consist of dacite and andesite rooted bodies and associated volcanoclastics, i.e., dacite vent breccia, andesite lava flows, and pyroclastics [32,34]. The Vent breccia unit was emplaced within the Upper Cretaceous flysch, and it was afterward pierced by dacite domes [32,33]. This unit was interpreted by [35] as a large maar-diatreme structure. The volcanic activity in Roșia Montană started with the Cetate dacite at  $13.65 \pm 0.63$  Ma [26] and continued with the Rotunda andesite at  $9.3 \pm 0.47$  Ma [36].

The Roșia Montană ore deposit was interpreted as a low-sulfidation one by [37] based on the morphology of the ore bodies, the ore and gangue mineralogy, the alteration mineral assemblages, the zonality of alterations around the ore bodies, and the geochemical associations. The fluid inclusion measurements carried out on magmatic and hydrothermal quartz, sphalerite, adularia, and apatite [38] revealed the low salinity ranging approximately from 1 to 4 wt% NaCl equiv., and the low to medium homogenization temperatures ranging from 198 to 300 °C, and exceptionally up to 340 °C, of the fluids in several ore bodies from Roșia Montană, confirming the LS character of the ore deposit.

These fluid inclusion data are in agreement with the homogenization temperatures obtained by [39] on two hydrothermal quartz generations from Cetate Breccia, i.e., 267 and 240 °C, and on quartz veins, with values ranging from 237 to 252 °C. The same author distinguished two gold mineral assemblages, i.e., (i) gold-sulfides-hydrothermal quartz with a  $T_h = 240\text{--}297$  °C, and (ii) gold-hydrothermal quartz with a  $T_h = 250\text{--}275$  °C. The Roșia Montană ore deposit was assigned to the IS type by [40], and this opinion was shared by [32], who interpreted the ore deposit as a mid to shallow-level intermediate sulfidation epithermal system.

However, based on cross-cutting relationships among different mineralized structures (veins and breccias), the authors in [6] distinguished four main ore deposition events in terms of gold and silver grades, ore and gangue mineralogy, and timing, i.e., (i) gold-rich early hydrothermal breccias with Ag-poor native gold, Ag-sulfosalts, scarce pyrite, and quartz-adularia gangue; (ii) gold-silver-rich veins with native gold, Ag sulfosalts,

scarce common sulfides, quartz, and adularia; (iii) Ag-Au hydrothermal breccias and veins with acanthite, Ag-sulfosalts, native silver, native gold, common sulfides, quartz, and adularia; and (iv) high-grade silver veins with Ag- and Au-Ag tellurides, Ag-Ge-Te sulfosalts, tetrahedrite, galena, sphalerite, chalcopyrite, native gold, rhodochrosite, adularia, and quartz.

These data coupled with the fluid inclusion data by [41] allowed [6] to infer a transition from an early LS environment with Au-dominant, Ag-subordinate ores to a final IS environment with dominant Ag, subordinate Au, and a significant Te and Ge signature. The same evolution from early LS to late IS characteristics at the ore-deposit scale was stated by [33]. The IS ore bodies demonstrated higher homogenization temperatures than the early LS ones and were correlated by [6] to late magmatic pulses.

The  $^{40}\text{Ar}$ - $^{39}\text{Ar}$  radiometric dating made on hydrothermal adularia by [33,41] and [42] in different sectors of the ore deposit revealed the existence of two distinct ages for ore deposition, the first one of  $13.17 \pm 0.08$  to  $13.24 \pm 0.10$  Ma, and the second one in the range of  $12.85 \pm 0.07$  Ma– $12.71 \pm 0.13$  Ma. These results suggest either a long-lasting ore deposition period of about 0.5 Ma, or two distinct metallogenic events.

### 3. Materials and Methods

New ore mineralogy and microchemical data on sphalerite were acquired on samples from the Roman underground mining networks from the southern part of the Cărnic massif, Roșia Montană, as follows: sample 1372 from Cărnic 4 Upper—stope D4; sample 1551 from Cărnic 10 Lower—adit G4; sample 1660 from Cărnic 10 Middle—pillar P7; and sample 2054 from Cărnic 1 Lower—stope D15. These ore samples were collected during the geological mapping of the Roman underground networks from Roșia Montană as part of the mining archaeological research program carried out from 1999 to 2013 [33,43,44] in the frame of the Roșia Montană mining project promoted by the Canadian mining company Gabriel Resources Ltd. [45]. Sample 3231 was collected from the Cărniceș vein in the Vercheș mining level (+853 m ASL).

Optical microscopy, scanning electron microscopy, and electron probe microanalyses were carried out at the GET laboratory from Paul Sabatier University, Toulouse, France and allowed the mineralogy identification of the Au-Ag ores and the microchemical characterization of the main ore minerals, including sphalerite. Preliminary SEM observations were made with a JSM-6360 electron microscope using a voltage of 20 kV. The microchemical data were acquired with a CAMECA SX50 electron microprobe using an acceleration voltage of 25 kV, a beam current of 20 nA, and a counting time of 10 s for peaks and 5 s for the background, as well as a 3 micrometer  $\times$  3 micrometer analyzed area.

The standards used were pure metals for As, Sb, Ag, Au, Se, Sn, and Te; chalcopyrite for S, Fe, and Cu; galena for Pb; sphalerite for Zn; CdS for Cd; and  $\text{MnTiO}_3$  for Mn. We used K alpha lines for S, Fe, Cu, Mn, Zn, and L; alpha lines for As, Sb, Cd, Ag, Au, Se, Sn, and Te; L beta lines for As; and M alpha lines for Pb. The calculated detection limits were 500 ppm for Mn, 550 ppm for S, 700 ppm for Cu, 700 ppm for Fe, 800 ppm for Sn, 800 ppm for Te, 800 ppm for Zn, 900 ppm for Cd, 900 ppm for Se, 1000 ppm for Sb, 1500 ppm for Ag, 2000 ppm for Au, 2700 ppm for Pb, and 4000 ppm for As.

The Au and Ag grades were obtained by the commercially available geochemical services provided by ALS Roșia Montană. The dataset used by the present study also includes EPMA results on sphalerite from the Roșia Montană ore deposit previously published by [6,23,35,46,47]. Additional microchemical data on sphalerite from the Cisma [48,49], Cavnic [50], Herja [51–53], and Toroioaga [46,53] ore deposits from the Baia Mare ore district (NW Romania) were also used.

### 4. Results

An underground geological observation and mineralogy study presented new ore deposit data for several sphalerite-bearing ore bodies from Roșia Montană. Sample 1372 was collected from a hydrothermal breccia dyke structure (Figure 2a) that belongs to the early

Au-rich LS ore deposition event separated by [6]. Indeed, the grades of the ore body ranged from several g/t gold and silver to 57.5 g/t Au and 45 g/t Ag (sample 1365), and rose up to 177 g/t Au and 133 g/t Ag (sample 1361).

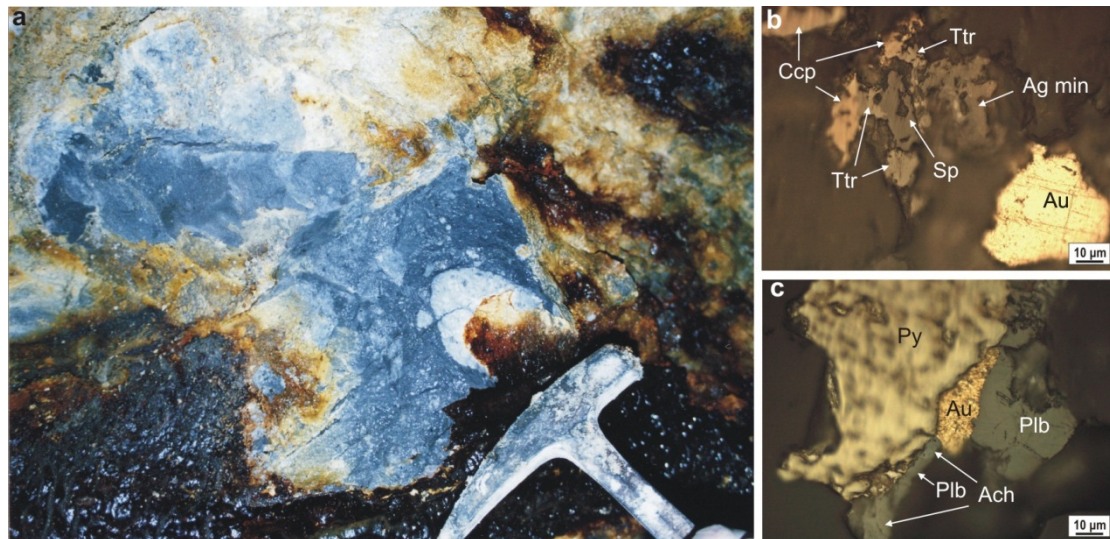


**Figure 2.** Underground view (a), and microphotographs in plane polarized light (b,c) of the ore body corresponding to sample 1372, the Roman mining network Cârnic 4, Upper sector: (a) detail of the breccia dyke ore body composed of two types of breccia, one consisting of black hydrothermal cement and scarce small-sized fragments (upper part) and the second with black fine matrix and angular to rounded dacite fragments (lower part); (b) native gold, chalcopyrite, sphalerite, tetrahedrite, and Ag-minerals optically identified as polybasite  $\pm$  acanthite within the hydrothermal cement; and (c) native gold, polybasite, and acanthite deposited on the pyrite grain. Abbreviations: Ach: acanthite; Ag min: Ag minerals; Au: native gold; Ccp: chalcopyrite; Plb: polybasite; Py: pyrite; Sp: sphalerite; and Ttr: tetrahedrite.

The native gold is hosted by hydrothermal cement and white quartz. It occurs as free grains in voids and is locally deposited onto and within the pyrite grains. The native gold is associated with scarce pyrite, minor sphalerite, and very minor chalcopyrite, as well as several Ag-minerals, likely polybasite and acanthite (Figure 2b,c). The native gold is covered and slightly corroded by the silver minerals (Figure 2c). The ore body and the host rock are highly silicified and intensely adularized.

Samples 1551 and 1660 were picked up from an ore body that consists of a hydrothermal breccia dyke with dacite fragments held together by black hydrothermal cement and massive to locally vuggy white quartz (Figure 3a), which is cut by several en échelon quartz veins. Sample 1551 was selected from the hydrothermal cement of the breccia dyke, and sample 1660 is a fragment from a quartz vein that cuts the breccia body.

The hydrothermal cement of the breccia contains native gold associated with Ag-minerals, e.g., polybasite, acanthite (Figure 3b), pyrite, sphalerite, chalcopyrite, galena, and tetrahedrite (Figure 3c). The ore grades obtained only on the hydrothermal breccia material without the overprinting quartz vein (sample 1551) were 7.94 g/t Au and 122 g/t Ag.

Sample 1660 was collected approximately 33-m NE from sample 1551, from a vertical safety pillar where the ore body exploited by the Roman miners is still preserved (Figure 4a). The sample consists of a quartz vein fragment that contains a continuous sequence of ore minerals, which cuts the breccia body. Overall, the main ore body composed of breccia dyke and the crosscutting quartz veins are LS; however, it shows a transition from the LS to the IS epithermal style, and it belongs to the third ore depositional event separated by [6].

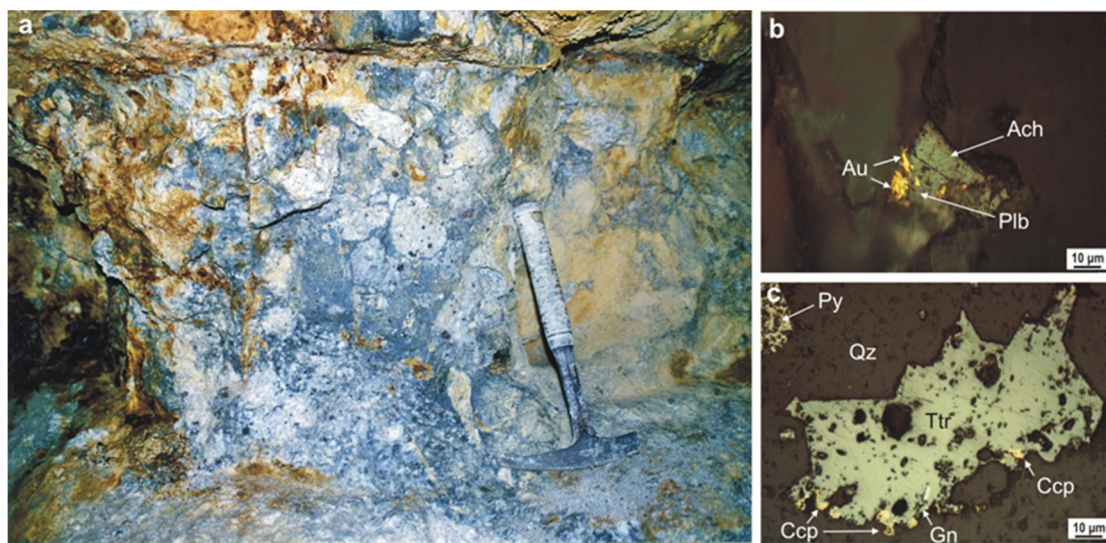


**Figure 3.** Underground view (a), and microphotographs in plane polarized light (b,c) of the ore body corresponding to sample 1551, the Roman mining network Cârnic 10, Lower sector: (a) partial view of a face line of the Roman stope with the hydrothermal breccia ore body with rounded to sub-angular rock fragments (mainly dacite) and black cement; (b) native gold associated to acanthite and polybasite deposited in a void of the hydrothermal cement; and (c) tetrahedrite grain associated to galena, chalcopyrite, and an isolated pyrite crystal. Ach: acanthite; Au: native gold; Ccp: chalcopyrite; Gn: galena; Plb: polybasite; Py: pyrite; Qz: quartz; and Ttr: tetrahedrite.

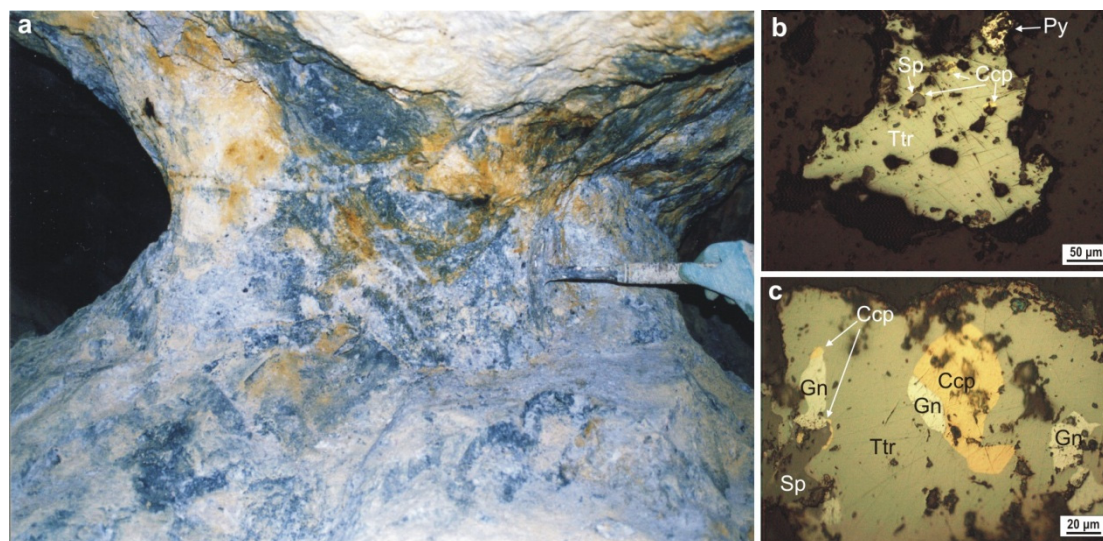


**Figure 4.** Underground view (a), and microphotographs in plane polarized light (b,c) of the ore body corresponding to sample 1660, the Roman mining network Cârnic 10, Middle sector: (a) eastern face of pillar P7 with a quartz vein cutting the hydrothermal breccia dyke; (b) tetrahedrite deposited in a void with associated chalcopyrite, sphalerite, and pyrite; and (c) tetrahedrite large grain with chalcopyrite, galena, and sphalerite inclusions. Abbreviations: Ccp: chalcopyrite; Gn: galena; Py: pyrite; Sp: sphalerite; and Ttr: tetrahedrite.

The ore body is intensely silicified and adularized. The grades of a bulk sample composed of hydrothermal breccia and the overprinting quartz vein located close to sample 1660 were 97.1 g/t Au and 54 g/t Ag (sample 1657). The ore microscopy study of sample 1660 revealed the occurrence of tetrahedrite, sphalerite, chalcopyrite, and pyrite (Figure 4b). The hydrothermal breccia dyke also contains native gold hosted by quartz, polybasite, and common sulfides (galena, sphalerite, and chalcopyrite).

Argyrodite associated to Ag-bearing tetrahedrite, polybasite, native gold, chalcopyrite, pyrite, and sphalerite was also reported by [54]. Another sample picked up from the same

ore body, approximately 15-m north-west, carries 12 g/t Au and 153 g/t Ag (sample 1713). This ore sample contains more abundant sulfides, with tetrahedrite, chalcopyrite, galena, and sphalerite (Figure 4c) associated with native gold and polybasite.

Sample 2054 was collected from a face line of a Roman stope that followed a hydrothermal breccia dyke structure (Figure 5a). The breccia is built out of black hydrothermal cement and white hydrothermal quartz, angular to sub-angular dacite fragments, and rounded to sub-rounded Cretaceous sandstone fragments. Locally, the hydrothermal cement contains visible pyrite crystals. The gold and silver grades of this ore body are elevated and constant from one sample to another, ranging from 33.1 g/t Au and 30 g/t Ag (sample 2010) to 133 g/t Au and 86 g/t Ag (sample 2017). The precious metals grade of the sample 2054 was 83.2 g/t Au and 75 g/t Ag.

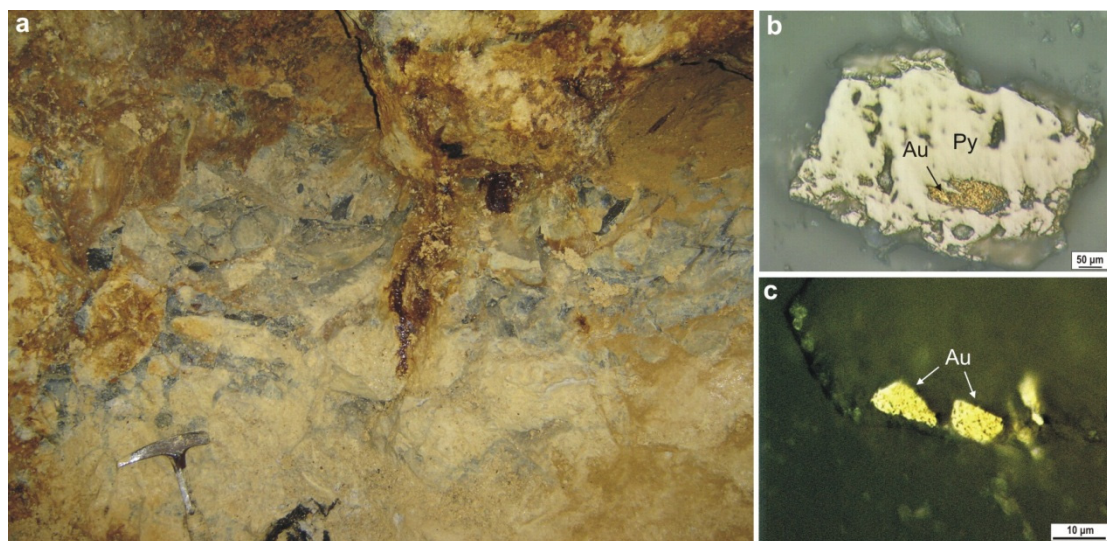


**Figure 5.** Underground view (a), and microphotographs in plane polarized light (b,c) of the ore body corresponding to sample 2054, the Roman mining network Cârnic 1, Lower sector; (a) detail of the breccia dyke ore body with angular dacite fragments and black hydrothermal cement; (b) native gold deposited within a pyrite crystal; and (c) native gold deposited within the voids of the hydrothermal cement. Abbreviations: Au: native gold; and Py: pyrite.

The ore microscopy study revealed the abundance of native gold and the coarse dimensions of the gold grains reaching up to 1.5 cm, such as continuous thin layers that occur as a distinct ore deposition sequence. Apart from native gold, the cement of the breccia contains pyrite that is abundant locally. Polybasite and scarce chalcopyrite and sphalerite are also present. Native gold occurs within pyrite (Figure 5b) as isolated grains within the hydrothermal cement (Figure 5c) and the white quartz or is deposited on the dacite fragments of the breccia.

The ore body and the host rock are silicified and adularized. The silicification halo extends on several tens of centimeters beyond the breccia dyke contact into the dacite host rock. The mineralogy of the ore and the associated alteration minerals assemblages suggest that this ore body is part of the early ore deposition event proposed by [6] and typically LS.

Sample 3231 was selected from a vein located in the Cârnicel massif. This so-called Cârnicel vein is part of the Silver Vein Group as mentioned by [55]. The vein is exposed in several tens of meters of the underground mining works, and it does not exceed 25 cm in width. The vein is banded with rhodochrosite sequences alternating with ore mineral sequences (Figure 6a). The ore mineral assemblage is dominated by tetrahedrite and sphalerite, which are associated to galena, chalcopyrite, hessite, and alburnite (Figure 6b,c). Additionally, native gold, sylvanite, altaite, pyrite, and marcasite were described for the same ore body by [6,23,56].

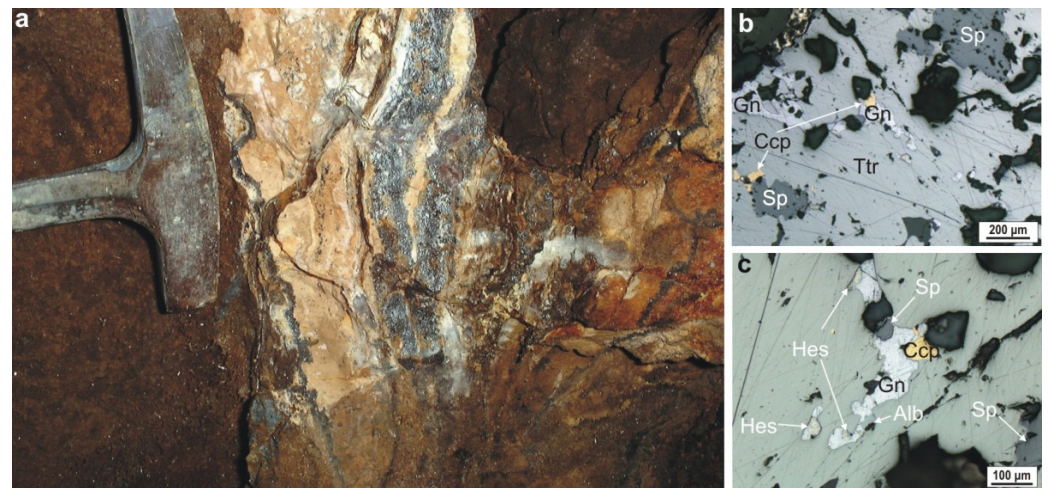


**Figure 6.** Underground view (a), and microphotographs in plane polarized light (b,c) of the ore body corresponding to sample 3231, Cârnicel vein, Vercheș mining level: (a) detail of the Cârnicel vein depicting the rhodochrosite and ore minerals sequences; (b) tetrahedrite dominated sulfide assemblage with sphalerite, galena, and chalcopyrite inclusions; and (c) detail of image 6b, showing galena and the associated chalcopyrite, hessite, and alburnite inclusions within the tetrahedrite. Abbreviations: Alb: alburnite; Ccp: chalcopyrite; Gn: galena; Hes: hessite; Sp: sphalerite; and Ttr: tetrahedrite.

The most abundant gangue mineral is rhodochrosite, whereas rhodonite, quartz, and adularia occur in small amounts [6]. The vein is hosted by the Vent breccia, and the hydrothermal alterations consist of adularization, carbonatation, minor silicification, and sericitization. The overall mineralogy indicates the IS character of the ore body. The similarities with other vein structures from the Cetate massif suggest its late deposition time during the hydrothermal system evolution.

The newly acquired geological information on the ore samples from Roșia Montană is summarized in Table 1 and allows us to distinguish the epithermal style of each ore body.

**Table 1.** The general characteristics of the epithermal ore bodies from Roșia Montană ore deposits with new EPMA data on sphalerite.

Sample ID	Mining Work	Ore Body and Alteration	Ore Mineral Assemblage	Epithermal Style
1372	C4 Upper-stope D4	hydrothermal breccia dyke and related hydrothermal cement injections with quartz and barite; silicification, adularia	Au-Py-Plb-Ach-Ccp-Sp-Ttr	LS
1551	C10 Lower-adit G4	hydrothermal breccia dyke; silicification, adularia	Au-Plb-Ach-Py-Sp-Ccp-Gn-Ttr	LS; transitional LS to IS
1660	C10 Middle-pillar P7	quartz vein cutting hydrothermal breccia dyke; silicification, adularia	Au-Plb-Gn-Sp-Ccp-Qz	LS; transitional LS to IS
2054	C1 Lower-stope D15	hydrothermal breccia dyke; silicification, adularia	Au-Py-Plb-Ccp-Sp-Fe hyd	LS
3231	Vercheș level, +853 m ASL	Cârnicel vein; banded vein with tellurides-base metals-gold and rhodochrosite gangue; adularia, carbonatation, minor silicification and sericitization	Ttr-Hes-Gn-Sp-Ccp-Alb-Rds-Qz	IS

Abbreviations: Ach: acanthite; Alb: alburnite; Au: native gold; Ccp: chalcopyrite; Fe hyd: Fe-hydroxides; Gn: galena; Hes: hessite; Plb: polybasite; Py: pyrite; Qz: quartz; Rds: rhodochrosite; Sp: sphalerite; and Ttr: tetrahedrite.

The EPMA data acquired on sphalerite from Roșia Montană are listed in Table 2 and show its low-Fe content (up to 0.53 wt%). The Mn content exceeds the Fe content and ranged from 1.19 to 6.01 wt%. The Cd and Cu content were up to 0.24 wt% and 0.45 wt%, respectively. The Sb level was very low, with only three values above the detection limit

(sample 1660). The Ag content was unusually high, in the 7.63–10.45 wt% range for one sample, and mostly below the detection limit for the remaining point analysis.

**Table 2.** The quantitative microchemical data (wt%) for sphalerite from the Roşia Montană ore deposit.

No.	Sample	LS/IS	Element (wt%)									Calculated Formula (Based on 2 apfu)
			S	Zn	Mn	Fe	Cu	Ag	Cd	Sb	Total	
1	1372-C2-2	LS	34.05	63.25	1.28	0.52	0.11	bdl	bdl	bdl	99.21	(Zn <sub>0.94</sub> Mn <sub>0.02</sub> Fe <sub>0.01</sub> ) $\Sigma$ = 0.97S <sub>1.03</sub>
2	1372-C2-3	LS	32.42	63.77	1.28	0.45	bdl	bdl	0.13	bdl	98.05	(Zn <sub>0.97</sub> Mn <sub>0.02</sub> Fe <sub>0.02</sub> ) $\Sigma$ = 1.00S <sub>1.00</sub>
3	2054-C2-6	LS	33.87	61.75	2.21	0.53	0.45	bdl	0.15	bdl	98.96	(Zn <sub>0.92</sub> Mn <sub>0.04</sub> Fe <sub>0.01</sub> Cu <sub>0.01</sub> ) $\Sigma$ = 0.97S <sub>1.03</sub>
4	RM 1551-C2-3	LS	33.64	58.72	4.38	0.11	0.41	bdl	0.14	bdl	97.39	(Zn <sub>0.88</sub> Mn <sub>0.08</sub> Cu <sub>0.01</sub> ) $\Sigma$ = 0.97S <sub>1.03</sub>
5	RM 1551-C2-8	LS	33.62	57.60	5.17	0.08	bdl	bdl	0.16	bdl	96.63	(Zn <sub>0.87</sub> Mn <sub>0.09</sub> ) $\Sigma$ = 0.97S <sub>1.03</sub>
6	1660-1-C5-9	LS	28.81	54.87	1.39	0.16	0.41	10.45	0.24	0.26	96.60	(Zn <sub>0.90</sub> Ag <sub>0.10</sub> Mn <sub>0.03</sub> Cu <sub>0.01</sub> ) $\Sigma$ = 1.04S <sub>0.96</sub>
7	1660-1-C5-10	LS	30.08	57.81	1.19	0.11	0.31	9.54	0.23	0.19	99.47	(Zn <sub>0.91</sub> Ag <sub>0.09</sub> Mn <sub>0.02</sub> Cu <sub>0.01</sub> ) $\Sigma$ = 1.03S <sub>0.97</sub>
8	1660-1-C5-11	LS	30.63	56.84	1.39	0.13	0.16	8.53	0.20	bdl	97.87	(Zn <sub>0.90</sub> Ag <sub>0.08</sub> Mn <sub>0.03</sub> ) $\Sigma$ = 1.01S <sub>0.99</sub>
9	1660-1-C5-13	LS	31.60	57.22	1.36	0.14	0.22	7.63	0.19	0.14	98.50	(Zn <sub>0.89</sub> Ag <sub>0.07</sub> Mn <sub>0.03</sub> ) $\Sigma$ = 1.00S <sub>1.00</sub>
10	1660-1-20	LS	34.23	61.39	4.44	0.09	0.01	bdl	0.16	bdl	100.33	(Zn <sub>0.90</sub> Mn <sub>0.08</sub> ) $\Sigma$ = 0.98S <sub>1.02</sub>
11	3231C_C1_7	IS	34.64	60.68	6.01	0.10	0.17	0.16	0.15	bdl	101.91	(Zn <sub>0.87</sub> Mn <sub>0.11</sub> ) $\Sigma$ = 0.98S <sub>1.02</sub>

Below detection limit values were obtained for Au, As, Pb, Se, Sn, and Te in all measured points; “bdl” = below detection limit.

## 5. Discussion

Sphalerite is the most common Zn sulfide, and it occurs in a wide variety of ore deposits as the main source of Zn. It has the capacity to host large amounts of minor and trace elements at levels that allow their economic recovery as by-products or may create environmental issues [46]. The chemical composition of sphalerite, mostly the Fe-content, was proven to be temperature and pressure-sensitive and was consequently used as geothermometer (e.g., [57–59]). The Fe content in sphalerite was also considered a distinctive feature between LS and IS epithermal ore deposits [3,5] as it is reflected by the macroscopic color of the mineral, which became a useful field observation.

The ore mineral assemblage of the studied ore samples from Roşia Montană contained sphalerite, irrespective of their LS or IS style. Samples 1372 and 2054 were collected from typical LS ore bodies with native gold, subordinate Ag-minerals (sulfide and sulfosalts), and scarce sulfides, with pyrite being the most abundant. The related hydrothermal alteration consisted of silicification and adularia. The gold grade of these ore bodies is generally greater than the silver grade and usually ranges in the level of tens of g/t. Samples 1551 and 1660 were collected from LS ore bodies showing a transitional character from LS to IS, with less native gold and more abundant Ag-minerals and common sulfides.

This change in mineralogy is reflected by the precious metal grades as well, with the Ag content being several times greater than the Au content. The alteration mineral assemblage remained the same with quartz and adularia. On the other hand, sample 3231 was collected from the IS Cărnicele vein. This ore body consists of abundant sulfides (tetrahedrite-tennantite, sphalerite, galena, and chalcopyrite), hessite, subordinate native gold, and minor Au-Ag-tellurides, altaite, argyrodite, and alburnite [6,23,60–62].

The hydrothermal alteration assemblage of this IS ore body was similar to that of the LS ones, with the extra occurrence of carbonatation and minor sericite. The IS ore bodies from Roşia Montană have abundant rhodochrosite gangue accompanied by minor Mn-pyroxenoid (rhodonite or pyroxmangite; [61]), which are absent from the LS ore bodies. The precious metal grades reported for the Cărnicele vein were 1.150 g/t Ag and 5 g/t Au [6], which are in agreement with the Ag:Au ratio > 100:1 of the IS deposits stated by [63].

The Fe content of the analyzed sphalerite from Roşia Montană was low, ranging from 0.08 to 0.53 wt% in LS ore bodies, and had a value of 0.10 wt% in the sample from the IS Cărnicele vein. These values are in contrast with the percent-level values of Mn, ranging from 1.19 to 5.17 wt% in the LS ore bodies and the 6.01 wt% value in the IS ore body. An even higher Mn content was reported for the sphalerite from the Cărnicele vein and another rhodochrosite vein in the Cetate massif, i.e., (in wt%), 4.98–6.13 by [6] and 4.45–6.76 by [46]. The Mn-rich environment of the IS veins from Roşia Montană is reflected (in addition to the abundance of rhodochrosite) by the higher Mn content in sphalerite. However, the



material) [46,48–53,67–70] suggest the existence of two major trends of the Fe-Mn ratio (Figure 7), (i.e., *9i*) the Mn-rich trend and (*ii*) the Fe-rich trend.

The Fe content was usually <1 wt% in the Mn-rich trend, and the Mn content was <0.75 wt% in the Fe-rich trend (Figure 7). In other words, high Fe values correlated to low Mn values and vice versa, with no coexisting intermediate values. There was a weak negative correlation between the Fe and Mn values; however, the distribution of the Fe and Mn values was discontinuous, with a clear gap between the maximum and the minimum value ranges.

The anomalously high Ag values in sphalerite from Roşia Montană (Table 2, sample 1660) ranging from 7.63 to 10.45 wt% were due to the presence of micrometric to sub-micrometric Ag-mineral inclusions. According to the review by [46], the amount of Ag that sphalerite may incorporate does not exceed several hundreds of ppm. Additionally, the occurrence of Ag-mineral microinclusions in the analyzed sphalerite is in agreement with the mineral assemblage containing Ag-bearing tetrahedrite, polybasite, and acanthite.

The available microchemical dataset for the sphalerite in LS and IS epithermal ore deposits from Romania (Figure 7) suggests that, at low Fe and Mn values, i.e., 2 and 1 wt%, respectively, there likely is a compositional field with a positive correlation between Fe and Mn, as was suggested by [50] who noticed the existence of a limited compositional field of sphalerite where a joint substitution may exist regarding Fe and Mn for Zn. The clear separation of the Mn-rich and the Fe-rich compositional trends with a gap of the values distribution between the maximum and minimum ranges confirms the partitioning between Fe and Mn in sphalerite as stated by [50].

Following the major contribution made by [3,5,63] in distinguishing the IS and LS epithermal ore deposit styles, the Fe content in sphalerite was considered to be a tool for differentiating the IS from LS ores, i.e., low Fe content in sphalerite from IS deposits, and high Fe content in sphalerite from LS deposits. However, [5] stated that these chemical peculiarities are, in fact, tendencies, not rules. Indeed, [63] indicated that the sphalerite in IS ore deposits contained from less than 1 to 10 mole percent FeS and locally up to 20 mole percent FeS, whereas the sphalerite in LS ore deposits contained from 1 to 15 mole percent FeS [5].

The chemical composition of sphalerite from the Apuseni Mountains generally shows low values of Fe in sphalerite in IS deposits and higher values in LS deposits; however, the highest Fe content in sphalerite is registered for the IS Haneş ore deposit (ca. 9 wt% or 16 mole percent FeS) [46], whereas the sphalerite from the LS ores in Roşia Montană have a Fe content ranging from approximately 0.1 to 8.5 wt% (0.2 to 15 mole percent FeS) [35,47].

The sphalerite from the IS ore deposits in the Baia Mare ore district shows a significant wider range of values for Fe as compared to the Apuseni Mountains, with the largest variation registered in the Herja ore deposit, from 1.78 to 12.90 wt% (3 to 23 mole percent FeS) [51–53,70], which exceeds the upper limit of 20 mole percent FeS in sphalerite from the IS ore deposits reported by [63].

The Mn content of sphalerite covers approximately the same range for LS and IS ore deposits, with higher values for the IS ores with rhodochrosite gangue from Roşia Montană (Figure 7). The IS veins from Săcărâmb frequently have rhodochrosite gangue, and the high-Mn content of sphalerite (4.97 wt%) reported by [46] was likely obtained on sphalerite associated with rhodochrosite. With the exception of Căvnic [50], the sphalerite from the Baia Mare ore district shows a low Mn content, with a maximum of 0.71 wt% for the Cisma ore deposit [48].

The Mn-richest sphalerite from the Baia Mare district, of up to 1.86 wt%, comes from the IS Pb-Zn-Cu and Au-Ag Căvnic ore deposit [50], where the veins have abundant rhodochrosite gangue. Apparently, higher Mn-contents in sphalerite in the IS ore bodies could be correlated to the presence of rhodochrosite gangue. However, the LS ore bodies without rhodochrosite gangue from Roşia Montană host sphalerite with an elevated Mn-content that ranges from 1.19 to 5.17 wt% (Table 2).

Based on EPMA and X-rays of the Fe, Mn, and Cd distribution mapping in zoned sphalerite crystals, the authors in [50] confirmed the coexistence of Fe-rich and Mn-rich sphalerite bands in a single crystal and concluded that the occurrence of Mn-rich or Fe-rich zones in sphalerite was determined by a “local” chemical control responsible for their incorporation. As such, when the sphalerite solid is enriched in Fe or in Mn, the other element gradually accumulates in the nearby hydrothermal fluid at the mineral-fluid interface.

The change in the chemistry of the precipitating sphalerite occurs when the excess of the first cation is consumed and the second cation begins to be chemisorbed and, consequently, the “external” factors, e.g., the ore formation conditions, have minor control. Accordingly, the Fe content in sphalerite appears to be a less reliable indicator for the epithermal style of the ore, as the EPMA dataset available for Romania also indicates.

## 6. Conclusions

The existence of the Fe-rich and the Mn-rich sphalerite compositional trends in the LS and IS epithermal ore deposits in Romania confirmed the competition between Fe and Mn substitution for Zn with a cation excluding the other one. This compositional pattern was found to be valid for both the Mn-dominant and the Fe-dominant substituents for Zn in sphalerite.

The distinction between the LS and IS epithermal style based on the Fe content in sphalerite from the epithermal deposits in Romania is only partial. Whereas, for the IS Măgura and Săcărâmb ore deposits in the Apuseni Mountains, the Fe content of sphalerite is low, on the contrary, for the IS ore deposits in the Baia Mare district and the Haneş deposit in the Apuseni Mountains, the Fe content is high. The sphalerite composition in Roşia Montană is also highly variable, irrespective of the LS or IS style of the host ore body. Consequently, the use of the Fe content of sphalerite as a distinctive feature between LS and IS ores does not appear to be reliable.

**Supplementary Materials:** The following are available online at <https://www.mdpi.com/article/10.3390/min11060634/s1>, Table S1. Quantitative microchemical data (wt%) for sphalerite from the epithermal ore deposits in the Apuseni Mountains; Table S2. Quantitative microchemical data (wt%) for sphalerite from the epithermal ore deposits in the Baia Mare ore district.

**Author Contributions:** Conceptualization, C.G.T. and M.P.A.; methodology, C.G.T. and M.P.A.; field work, C.G.T. and B.C.; data processing, C.G.T., M.P.A. and S.D.; validation, M.P.A. and C.G.T.; investigation, C.G.T.; data curation, M.P.A., C.G.T. and S.D.; original draft preparation, C.G.T., M.P.A., R.K. and S.D.; review and editing, C.G.T., R.K., M.P.A., S.D. and B.C.; visualization, M.P.A. and R.K.; supervision, C.G.T.; funding acquisition, B.C., C.G.T. and M.P.A. All authors have read and agreed to the published version of the manuscript.

**Funding:** The APC was funded by the doctoral grant of M.P.A., by the grant AGC 33442/10.09.2020, University Babeş-Bolyai (C.G.T.), and by the University Babeş-Bolyai contracts 6531/23.06.2020 and 4323/26.03.2019.

**Data Availability Statement:** The Data presented in this study are available in the submitted article and Supplementary Materials.

**Acknowledgments:** Thanks are addressed to the mining company Roşia Montana Gold Corporation for supporting the field work. Many thanks are addressed to Thierry Aigouy and Philippe de Parseval (Paul Sabatier University, Toulouse, France) and to Adrian Minuţ (RMGC, Romania). The linguistic revision by Mirela Mircea is highly appreciated.

**Conflicts of Interest:** The author Reka Kovacs is an employee of MDPI; however, she was not working for the journal Minerals at the time of submission and publication.

## References

1. Heald, P.; Foley, N.K.; Hayba, D.O. Comparative anatomy of volcanic-hosted epithermal deposits: Acid-sulfate and adularia-sericite types. *Econ. Geol.* **1987**, *82*, 1–26. [[CrossRef](#)]
2. Hedenquist, J.W. Mineralization Associated with Volcanic-Related Hydrothermal Systems in the Circum-Pacific Basin. In Proceedings of the Transactions of the Fourth Circum-Pacific Energy and Mineral Resources Conference, Singapore, 17–22 August 1986; pp. 513–524.
3. Hedenquist, J.W.; Arribas, A.; Gonzalez-Urrien, E.J. Exploration for epithermal gold deposits. *Rev. Econ. Geol.* **2000**, *13*, 245–277.
4. John, D.A. Magmatic influence on characteristics of Miocene low-sulfidation Au-Ag deposits in the northern Great Basin. *Geol. Soc. Am. Abstr. Progr.* **1999**, *31*, A-405.
5. John, D.A. Miocene and early Pliocene epithermal gold-silver deposits in the northern Great Basin, western United States: Characteristics, distribution, and relationship to Magmatism. *Econ. Geol.* **2001**, *96*, 1827–1853. [[CrossRef](#)]
6. Tămas, C.I.G.; Bailly, L.; Ghergari, L.I.; O'Connor, G.; Minut, A. New occurrences of tellurides and argyrodite in roșia montană, Apuseni mountains, Romania, and their metallogenic significance. *Can. Mineral.* **2006**, *44*, 367–383. [[CrossRef](#)]
7. Lang, B. The base metals-gold hydrothermal ore deposits of Baia Mare, Romania. *Econ. Geol.* **1979**, *74*, 1336–1351. [[CrossRef](#)]
8. Borcos, M.; Krautner, H.G.; Udubașa, G.; Săndulescu, M.; Năstăseanu, S.; Bițoiianu, C. *Harta Substanțelor Minerale Utile*, 2nd ed.; Institutul de Geologie și Geofizică: Bucharest, Romania, 1983.
9. Borcos, M.; Krautner, H.G.; Udubașa, G.; Săndulescu, M.; Năstăseanu, S.; Bițoiianu, C. *Map of the Mineral Resources*, 2nd ed.; Institute of Geology and Geophysics: Bucharest, Romania, 1984.
10. Bailly, L.; Milesi, J.-P.; Leroy, J.; Marcoux, E. Les minéralisations épithermales à Au-Cu-Zn-Sb du district de Baia Mare (Nord Roumanie): Nouvelles données minéralogiques et microthermométriques. *C. R. Acad. Sci. Ser. IIA Earth Planet. Sci.* **1998**, *327*, 385–390. [[CrossRef](#)]
11. Grancea, L.; Bailly, L.; Leroy, J.; Banks, D.; Marcoux, E.; Milési, J.; Cuney, M.; André, A.; Istvan, D.; Fabre, C. Fluid evolution in the Baia Mare epithermal gold/polymetallic district, Inner Carpathians, Romania. *Miner. Depos.* **2002**, *37*, 630–647. [[CrossRef](#)]
12. Ianovici, V.; Borcoș, M.; Bleahu, M.; Patrușiu, D.; Lupu, M.; Dimitrescu, R.; Savu, H. *The Geology of the Apuseni Mountains*; Editura Academiei: Bucharest, Romania, 1976; p. 631.
13. Bleahu, M.; Lupu, M.; Patrușiu, D.; Bordea, S.; Stefan, A.; Panin, S. The structure of the Apuseni Mountains. In Proceedings of the XIIth Congress of the Carpatho-Balkan Geological Association, Bucharest, Romania, 8–13 September 1981; p. 107.
14. Săndulescu, M. *Geotectonica României*; Ed. Tehnica: Bucharest, Romania, 1984; p. 336.
15. Dimitrescu, R. Apuseni Mountains. In *Apuseni Mountains. Precambrian in Younger Fold Belts*; Zoubek, V., Ed.; Wiley: Chichester, UK, 1988; pp. 665–673.
16. Balintoni, I. Structure of the Apuseni Mountains. *Rom. J. Tecton. Reg. Geol.* **1994**, *75*, 51–58.
17. Balintoni, I. *Geotectonica Terenurilor Metamorfice Din Romania*; Carpatica: Cluj-Napoca, Romania, 1997; p. 176.
18. Dallmeyer, R.D.; Pană, D.I.; Neubauer, F.; Erdmer, P. Tectonothermal Evolution of the Apuseni Mountains, Romania: Resolution of Variscan versus Alpine Events with <sup>40</sup>Ar/<sup>39</sup>Ar Ages. *J. Geol.* **1999**, *107*, 329–352. [[CrossRef](#)]
19. Pană, D.I.; Heaman, L.M.; Creaser, R.A.; Erdmer, P. Pre-Alpine Crust in the Apuseni Mountains, Romania: Insights from Sm-Nd and U-Pb Data. *J. Geol.* **2002**, *110*, 341–354. [[CrossRef](#)]
20. Benea, M.; Tămaș, C.G. Neogene volcanics in the Apuseni Mts.: Historical mining and gold deposits. *Acta Miner. Petrogr. Field Guide Ser.* **2010**, *21*, 1–28.
21. Boștinescu, S. Porphyry copper systems in the South Apuseni Mountains, Romania. *Anu. Inst. Geol. Si Geofiz.* **1984**, *54*, 163–175.
22. Apopei, A.I.; Damian, G.; Buzgar, N.; Buzatu, A. Mineralogy and geochemistry of Pb-Sb/As-sulfosalts from Coranda-Hondol ore deposit (Romania)—Conditions of telluride deposition. *Ore Geol. Rev.* **2016**, *72*, 857–873. [[CrossRef](#)]
23. Tămas, C.G.; Grobety, B.; Bailly, L.; Bernhardt, H.-J.; Minuț, A. Alburnite, Ag<sub>8</sub>GeTe<sub>2</sub>S<sub>4</sub>, a new mineral species from the Roșia Montana Au-Ag epithermal deposit, Apuseni Mountains, Romania. *Am. Miner.* **2014**, *99*, 57–64. [[CrossRef](#)]
24. Ghițulescu, T.P.; Socolescu, M. Etude géologique et minière des Monts Métallifères (Quadrilatère aurifère et régions environnantes). *Annu. Inst. Géol. Roum.* **1941**, *21*, 181–463.
25. Rosu, E.; Seghedi, I.; Downes, H.; Alderton, D.H.M.; Szakács, A.; Pécskay, Z.; Panaiotu, C.; Panaiotu, E.C.; Nedelcu, L. Extension-related Miocene calc-alkaline magmatism in the Apuseni Mountains, Romania: Origin of magmas. *Schweiz. Mineral. Und Petrogr. Mitt.* **2004**, *84*, 153–172.
26. Roșu, E.; Udubașa, G.; Pécskay, Z.; Panaiotu, C.; Panaiotu, C.E. Timing of Miocene—Quaternary magmatism and metallogeny in the South Apuseni Mountains, Romania. In Proceedings of the Rom. Journal Mineral Deposit: “Fourth National Symposium on Economic Geology—Gold in Metaliferi Mountains”, Alba Iulia, Romania, 3–5 September 2004; pp. 33–38.
27. Neubauer, F.; Lips, A.; Kouzmanov, K.; Lexa, J.; Ivășcanu, P. 1: Subduction, slab detachment and mineralization: The Neogene in the Apuseni Mountains and Carpathians. *Ore Geol. Rev.* **2005**, *27*, 13–44. [[CrossRef](#)]
28. Udubașa, G.; Rosu, E.; Seghedi, I.; Ivășcanu, P.M. The “Golden Quadrangle” in the Metaliferi Mts., Romania: What does this really mean? In Proceedings of the Geodynamics and Ore Deposit Evolution of the Alpine-Balkan-Carpathian-Dinaride Province. ABCD—GEODE 2001, Workshop Vața Băi, Romania, 8–12 June 2001; pp. 3–23.
29. Kouzmanov, K.; von Quadt, A.; Peytcheva, I.; Harris, C.; Heinrich, C.A.; Rosu, E.; O'Connor, G. Rosia Poieni porphyry Cu-Au and Rosia Montana epithermal Au-Ag deposits, Apuseni Mts., Romania: Timing of magmatism and related mineralization. In Proceedings of the Au-Ag-Te-Se Deposits: IGCP 486 Field Workshop, Kiten, Bulgaria, 14–19 September 2005; Cook, N.J.,

- Bonev, I.K., Eds.; Bulgarian Academy of Sciences, Geochemistry, Mineralogy and Petrology: Sofia, Bulgaria, 2005; Volume 43, pp. 113–117.
30. Ivascanu, P.; Baker, T.; Lewis, P.; Kulcsar, Z.; Denes, R.; Tamas, C. Bolcana, Romania: Geology and discovery history of a gold rich porphyry deposit. In Proceedings of the 2019 NewGenGold Conference, Perth, Australia, 12–13 November 2019; pp. 145–160.
31. Udubasa, G.; Strusievcz, R.O.; Dafin, E.; Verdeş, G. Excursion Guide. Mineral Occurrences in the Metaliferi Mountains, Romania. *Rom. J. Miner.* **1992**, *75*, 35.
32. Leary, S.; O'Connor, G.; Minuț, A.; Tămaș, C.; Manske, S.; Howie, K. The Roșia Montană ore deposit. In *Au–Ag–Telluride Deposits of the Golden Quadrilateral, South Apuseni Mts., Romania*; Cook, N.J., Cristiana, L.C., Eds.; Romania Guidebook of the International Field Workshop of IGCP Project 486; IAGOD: Alba Iulia, Romania, 2004; pp. 89–98.
33. Manske, S.L.; Hedenquist, J.W.; O'Connor, G.; Tămaș, C.G.; Cauuet, B.; Leary, S.; Minuț, A. Roșia Montana, Romania: Europe's largest gold deposit. *Soc. Econ. Geol. Newsl.* **2006**, *64*, 9–15.
34. Bordea, S.; Ștefan, A.; Borcoș, M. *Harta Geologică a României, Scara 1:50,000, Foaia Abrud*; Institutul de Geologie și Geofizică: Bucharest, Romania, 1979.
35. Tămaș, C.G. *Structuri de Breccii Endogene (Breccia Pipe—Breccia Dyke) și Petrometalogenia Zăcământului Roșia Montană (Munții Metaliferi, România)*; Editura Casa Cărții de Știință: Cluj-Napoca, Romania, 2007.
36. Roșu, E.; Pécskay, Z.; Ștefan, A.; Popescu, G.; Panaiotu, C.; Panaiotu, C.E. The evolution of the Neogene volcanism in the Apuseni Mountains (Romania): Constraints from new K-Ar data. *Geol. Carpath.* **1997**, *48*, 353–359.
37. Mârza, I.; Tămaș, C.; Ghergari, L. Low sulfidation epithermal gold deposits from Roșia Montană, Metaliferi Mountains, Romania. *Stud. Cercet. Geol.* **1997**, *43*, 3–12.
38. Tămaș, C.G.; Bailly, L. Roșia Montană low-sulfidation ore deposit—Evidence from fluid inclusion study. *Stud. Univ. Babeș Bolyai Geol.* **1999**, *XLIV*, 49–56.
39. Borcoș, M. Observații în legătură cu determinarea condițiilor termodinamice de formare a unor zone mineralizate și a unor zăcăminte hidrotermale din Munții Metaliferi (II). *Stud. Cercet. Geol. Geofiz. Geogr. Ser. Geol.* **1968**, *13*, 93–111.
40. Sillitoe, R.H.; Hedenquist, J.W. Linkages between volcanotectonic settings, ore–fluid compositions, and epithermal precious-metals deposits. In *Volcanic, Geothermal and Ore-Forming Fluids: Rulers and Witnesses of Processes within the Earth*; Simmons, S.F., Graham, I.J., Eds.; Society of Economic Geologists, Special Publication: Littleton, CO, USA, 2003; pp. 315–343.
41. Manske, S.; Ullrich, T.; Reynolds, J.; O'Connor, G.V. Vein sets and hydrothermal alteration in the Cetate-Carnic Area, Roșia Montană district, Romania. *Rom. J. Miner. Depos.* **2004**, *81*, 122–125.
42. Wallier, S.; Rey, R.; Kouzmanov, K.; Pettke, T.; Heinrich, C.A.; Leary, S.; O'Connor, G.; Tamas, C.G.; Vennemann, T.; Ullrich, T. Magmatic Fluids in the Breccia-Hosted Epithermal Au-Ag Deposit of Rosia Montana, Romania. *Econ. Geol.* **2006**, *101*, 923–954. [[CrossRef](#)]
43. Cauuet, B.; Ancel, B.; Rico, C.; Tămaș, C. Ancient mining networks. In *The French Archaeological Missions 1999–2001*; Damian, P., Ed.; Mega Publishing House: Cluj-Napoca, Romania, 2003; pp. 467–526.
44. Cauuet, B.; Tămaș, C.G. *Les Travaux Miniers Antiques de Rosia Montana (Roumanie)*; Apports Croisés Entre Archéologie et Géologie: Madrid, Spain, 2012; Volume 128, pp. 219–241.
45. Resources, G. A Project or Romania. Available online: <http://www.gabrielresources.com/site/projects.aspx> (accessed on 22 April 2021).
46. Cook, N.J.; Ciobanu, C.L.; Pring, A.; Skinner, W.; Shimizu, M.; Danyushevsky, L.; Saini-Eidukat, B.; Melcher, F. Trace and minor elements in sphalerite: A LA-ICPMS study. *Geochim. Cosmochim. Acta* **2009**, *73*, 4761–4791. [[CrossRef](#)]
47. Drăgușanu, S. Mineralizații Auro-Argentifere din Nordul Zăcământului Roșia Montană, Munții Apuseni, România. Ph.D. Thesis, Babeș-Bolyai University, Cluj-Napoca, Romania, 2017.
48. Plotinskaya, O.Y.; Prokofiev, V.Y.; Damian, G.; Damian, F.; Lehmann, B. The Cisma de posit, Băiuț district, Eastern Carpathians, Romania: Sphalerite composition and formation conditions. *Carpathian J. Earth Environ. Sci.* **2012**, *7*, 265–273.
49. Kovács, R.; Tămaș, C.G. Cu<sub>3</sub>(As,Sb)<sub>4</sub> minerals from the Baia Mare metallogenic district, Eastern Carpathians, Romania—A case study from the Cisma ore deposit. *Geol. Q.* **2020**, *64*, 263–274. [[CrossRef](#)]
50. Di Benedetto, F.; Bernardini, G.P.; Costagliola, P.; Plant, D.; Vaughan, D.J. Compositional zoning in sphalerite crystals. *Am. Mineral.* **2005**, *90*, 1384–1392. [[CrossRef](#)]
51. Damian, G. Studiul Mineralogic, Geochimic și Genetic al Zăcământului Polimetalic de la Herja. Ph.D. Thesis, Universitatea București, București, România, 1996.
52. Cook, N.J.; Damian, G. New data on “plumosite” and other sulphosalt minerals from the Herja hydrothermal vein deposit, Baia Mare District, Rumania. *Geol. Carpath.* **1997**, *48*, 387–399.
53. George, L.L.; Cook, N.J.; Ciobanu, C.L. Partitioning of trace elements in co-crystallized sphalerite–galena–chalcopyrite hydrothermal ores. *Ore Geol. Rev.* **2016**, *77*, 97–116. [[CrossRef](#)]
54. Tămaș, C.G.; Cauuet, B.; Munoz, M. Argyrodite occurrence in Rosia Montana epithermal Au-Ag deposit, Apuseni Mountains, Romania—EPMA Data. *Rom. J. Miner. Depos.* **2016**, *89*, 7–12.
55. Brana, V. *Zăcămintele Metalifere ale Subsolului Românesc*; Editura Științifică: Bucharest, Romania, 1958; p. 261.
56. Cook, N.J.; Ciobanu, C.L.; Damian, G.; Damian, F. Tellurides and sulphosalts from deposits in the Golden Quadrilateral. In *Au-Ag-Telluride Deposits of the Golden Quadrilateral, South Apuseni Mts., Romania*; Cook, N.J., Ciobanu, C.L., Eds.; Guidebook of the International Field Workshop of IGCP Project 486; IAGOD: Alba Iulia, Romania, 2004; pp. 111–144.

57. Kullerud, G. The FeS-ZnS system a geological thermometer. *Nor. Geol. Tidsskr.* **1953**, *32*, 61–147.
58. Barton, P.B.; Toulmin, P. Phase relations involving sphalerite in the Fe-Zn-S system. *Econ. Geol.* **1966**, *61*, 815–849. [[CrossRef](#)]
59. Scott, S.D.; Barnes, H.L. Sphalerite geothermometry and geobarometry. *Econ. Geol.* **1971**, *66*, 653–669. [[CrossRef](#)]
60. Tămaş, C.G.; Bailly, L.; Cauuet, B. Breccia structures and Au-Ag mineral assemblages in Roşia Montană ore deposit, Apuseni Mountains, Romania. In *Au–Ag–Telluride Deposits of the Golden Quadrilateral, South Apuseni Mts., Romania*; Cook, N.J., Ciobanu, C.L., Eds.; Guidebook of the International Field Workshop of IGCP Project 486; IAGOD: Alba Iulia, Romania, 2004; pp. 254–255.
61. Ciobanu, C.L.; Cook, N.J.; Tămaş, C.; Leary, S.; Manske, S.; O'Connor, G.; Minuţ, A. Tellurides-gold-base metal association at Roşia Montană: The role of hessite as gold carrier. In *Au–Ag–Telluride Deposits of the Golden Quadrilateral, South Apuseni Mts., Romania*; Guidebook of the International Field Workshop of IGCP Project 486; Cook, N.J., Ciobanu, C.L., Eds.; IAGOD: Alba Iulia, Romania, 2004; pp. 187–202.
62. Ciobanu, C.L.; Gabudeanu, B.; Cook, N.J. Neogene ore deposits and metallogeny of the Golden Quadrilateral, South Apuseni Mountains, Romania. In *Au–Ag–Telluride Deposits of the Golden Quadrilateral, South Apuseni Mts., Romania*; Cook, N.J., Ciobanu, C.L., Eds.; Guidebook of the International Field Workshop of IGCP Project 486; IAGOD: Alba Iulia, Romania, 2004; pp. 23–88.
63. Einaudi, M.T.; Hedenquist, J.W.; Inan, E.E. Sulfidation state of fluids in active and extinct hydrothermal systems: Transition from porphyry to epithermal environments. *SEG Spec. Publ.* **2003**, *10*, 285–314.
64. Olivo, G.R.; Gibbs, K. Paragenesis and mineral chemistry of alabandite (MnS) from the Ag-rich Santo Toribio epithermal deposit, Northern Peru. *Miner. Mag.* **2003**, *67*, 95–102. [[CrossRef](#)]
65. Makovicky, E. Crystal Structures of Sulfides and Other Chalcogenides. *Rev. Miner. Geochem.* **2006**, *61*, 7–125. [[CrossRef](#)]
66. Tomashyk, V.F.; Feychuk, P.; Scherbak, L. *Ternary Alloys Based on II-VI Semiconductor Compounds*; CRC Press: Boca Raton, FL, USA, 2013; p. 526.
67. Buzatu, A.; Buzgar, N.; Damian, G.; Vasilache, V.; Apopei, A.I. The determination of the Fe content in natural sphalerites by means of Raman spectroscopy. *Vib. Spectrosc.* **2013**, *68*, 220–224. [[CrossRef](#)]
68. Buzatu, A.; Damian, G.; Dill, H.G.; Buzgar, N.; Apopei, A.I. Mineralogy and geochemistry of sulfosalts from Baia Sprie ore deposit (Romania)—New bismuth minerals occurrence. *Ore Geol. Rev.* **2015**, *65*, 132–147. [[CrossRef](#)]
69. Damian, G.; Buzatu, A.; Apopei, I.A.; Szakács, Z.L.; Denuş, I.; Iepure, G.; Bărgăoanu, D. Valentinite and Colloform Sphalerite in Epithermal Deposits from Baia Mare Area, Eastern Carpathians. *Minerals* **2020**, *10*, 121. [[CrossRef](#)]
70. Tămaş, C.G.; Mârza, I.; Har, N.; Denuş, I. The black calcite and its mineral assemblage in Herja ore deposit, Romania. *Eur. J. Miner.* **2018**, *30*, 1141–1153. [[CrossRef](#)]